



HAL
open science

Excitons in CdTe/ZnTe heterostructure with atomically thin CdTe layers

N. Filosofov, A. Yu. Serov, G. Karczewski, V. Agekian, H. Mariette, V. Kochereshko

► **To cite this version:**

N. Filosofov, A. Yu. Serov, G. Karczewski, V. Agekian, H. Mariette, et al.. Excitons in CdTe/ZnTe heterostructure with atomically thin CdTe layers. *AIP Advances*, 2020, 10 (8), pp.085224. 10.1063/5.0012146 . hal-03196297

HAL Id: hal-03196297

<https://hal.science/hal-03196297>

Submitted on 25 Aug 2023

HAL is a multi-disciplinary open access archive for the deposit and dissemination of scientific research documents, whether they are published or not. The documents may come from teaching and research institutions in France or abroad, or from public or private research centers.

L'archive ouverte pluridisciplinaire **HAL**, est destinée au dépôt et à la diffusion de documents scientifiques de niveau recherche, publiés ou non, émanant des établissements d'enseignement et de recherche français ou étrangers, des laboratoires publics ou privés.

Excitons in CdTe/ZnTe heterostructure with atomically thin CdTe layers

Cite as: AIP Advances 10, 085224 (2020); doi: 10.1063/5.0012146

Submitted: 10 July 2020 • Accepted: 3 August 2020 •

Published Online: 18 August 2020



N. G. Filosofov,¹ A. Yu. Serov,¹ G. Karczewski,² V. F. Agekian,¹ H. Mariette,³ and V. P. Kochereshko^{4,a)}

AFFILIATIONS

¹St. Petersburg State University, 199034 St. Petersburg, Russia

²Institute of Physics, Polish Academy of Sciences, PL-02-668 Warsaw, Poland

³Institut Neel CNRS, 38042 Grenoble, France

⁴Ioffe Institute, Russian Academy of Sciences, 194021 St. Petersburg, Russia

^{a)}Author to whom correspondence should be addressed: Vladimir.Kochereshko@mail.ioffe.ru

ABSTRACT

Heterostructures with atomically thin double quantum wells based on CdTe/ZnTe are investigated by optical spectroscopy (photoluminescence and reflectivity methods) as a function of temperature and density of excitation. Heavy and light exciton luminescence lines are observed with comparable intensities and different temperature behaviors (they cross each other at about 65° K). All these features agree with a complete calculation that takes into account both a very small chemical band offset for such monolayer CdTe inclusions in the ZnTe matrix (namely, 2%), and, consequently, the importance of Coulombic interaction in these double quantum wells.

© 2020 Author(s). All article content, except where otherwise noted, is licensed under a Creative Commons Attribution (CC BY) license (<http://creativecommons.org/licenses/by/4.0/>). <https://doi.org/10.1063/5.0012146>

INTRODUCTION

Semiconductor compounds A_2B_6 , in particular CdTe and ZnTe, are often used for basic research as a model object. Unfortunately, the range of their device applications is not very wide because of rapid degradation. At the same time, they have a high structural quality and exhibit unique optical properties. It would be desirable to find opportunities for their wider practical use.

One of the reasons that limit the practical use of these compounds and related heterostructures is the noticeable mismatch of their crystal lattices. As a result, mechanical stresses arise on the interfaces, which ultimately lead to the degradation of the structure. Heterostructures with ultrathin quantum wells, in which two lattices “adapt” to each other, are free from this drawback.¹ However, due to mismatch of the lattices, the value of the band offset is known quite approximately. Hence, the scatter of published data on the offset in the valence band in CdTe/ZnTe heterostructures reaches $\pm 10\%$ of the total band offset.^{2,3} The situation with structures containing ultrathin, monoatomic layers is even more uncertain. For such structures, the very concept of band offset becomes vague.^{4,5}

The band offset consists of the chemical band offset, which is determined by the chemical composition of the interface, and the deformation band offset, which is associated with the elastic energy at the interface between the materials in contact. In accordance with the “common anion/cation” rule, the offset in the valence band should be small for structures with a common anion. Deformation can further reduce this band offset and even lead to the formation of a type-II structure.⁶ In this case, the main contribution for quantization of the hole energy is its Coulomb interaction with the electron.

Detailed experimental study of the photoluminescence (PL) spectra of CdTe/ZnTe structures with atomically thin quantum wells is carried out in this work. In contrast to previous studies (see, for example, Refs. 7 and 8) dealing with such atomic thin CdTe insertions into ZnTe, two peaks are observed here in the photoluminescence spectra, clearly attributed to heavy excitons mainly localized in CdTe layers and light ones mainly located in ZnTe. As a result, it was possible to clarify the values of the band offset in the valence band for such structures and to determine some parameters of excitons.

EXPERIMENT

The studied samples were grown by molecular beam epitaxy on (001) GaAs substrates. They consist of an about $1\ \mu$ thick ZnTe epitaxial layer in which two Cd atom monolayers are inserted. The distance between the CdTe layers is five monolayers of ZnTe, i.e., about 1.5 nm. To ensure high quality of the monolayers of CdTe and accurate thickness of the ZnTe spacer, this part of the structure was grown by the mode of atomic layer epitaxy.⁵

The two monoatomic CdTe layers form two tunnel bound delta-shaped quantum wells for photoexcited carriers in the ZnTe matrix. The reflection and photoluminescence (PL) spectra were registered at temperatures from 5 K to 100 K and at different intensities of optical excitation from $1\ \text{W}/\text{cm}^2$ to $80\ \text{W}/\text{cm}^2$. The PL spectra were excited by lasers with a wavelength of 473 nm for above-barrier excitation and with a wavelength of 532 nm for below-barrier excitation.

Figure 1 shows the reflection and PL spectra obtained at a temperature of 5 K. The features in the reflection and PL spectra coincide, which indicates that PL peaks at an energy of 2.28 eV are associated with the intrinsic states of the structure. It is in good agreement with the single peak reported in Ref. 8 at the same energy for a similar sample (two monolayers of CdTe into ZnTe) but without the splitting clearly present here.

A sharp feature in the reflection at 2.37 eV is related to the exciton transition in ZnTe layers. At first glance, the lines at 2.28 eV would be expected to correspond to the symmetric state. The asymmetric state of the exciton in these wells should be at energies above the barriers. We attribute a PL peak at 2.31 eV to the excited state of the exciton. At weak optical excitation, a broad band associated with donor-acceptor recombination is observed at an energy of 2.25 eV.

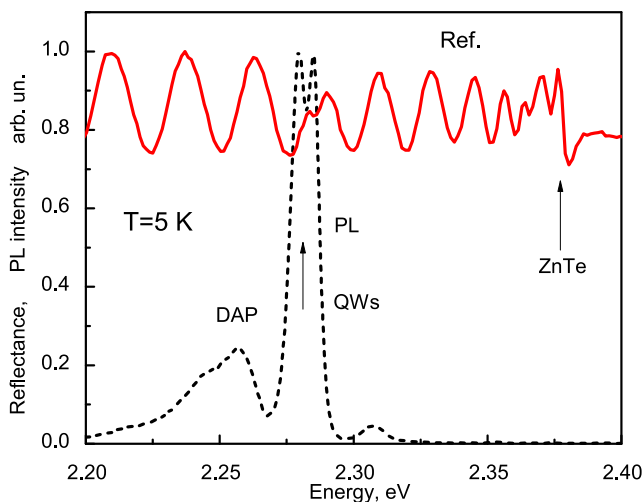


FIG. 1. Photoluminescence spectrum (short-dashed line) at the optical excitation with an intensity of $50\ \text{W}/\text{cm}^2$ and the reflection spectrum (solid line) at a temperature of 5 K. Exciton resonances in the barriers are indicated as (ZnTe). The photoluminescence lines (QWs) are associated with an exciton in a double quantum well. The photoluminescence broad band (DAP) refers to donor-acceptor recombination.

Figure 1

The doublet of the emission lines observed at energy of 2.28 eV has a linewidth of about 6 meV at a temperature of 5 K. Under the above-barrier excitation of extremely low density ($\sim 1\ \text{W}/\text{cm}^2$), the integral intensity of the short-wave component of this doublet is about two times larger than the long-wave component [Fig. 2(a)]. With an increase in the intensity of optical excitation, the PL signal is redistributed from the short-wave line to the long-wave one. At a pump intensity of $60\ \text{W}/\text{cm}^2$, the long-wave component is two times larger than the short-wave component. At weak below-barrier excitation ($\sim 20\ \text{W}/\text{cm}^2$), the intensity of the long-wave component of the doublet is 20% lower than the intensity of the short-wave

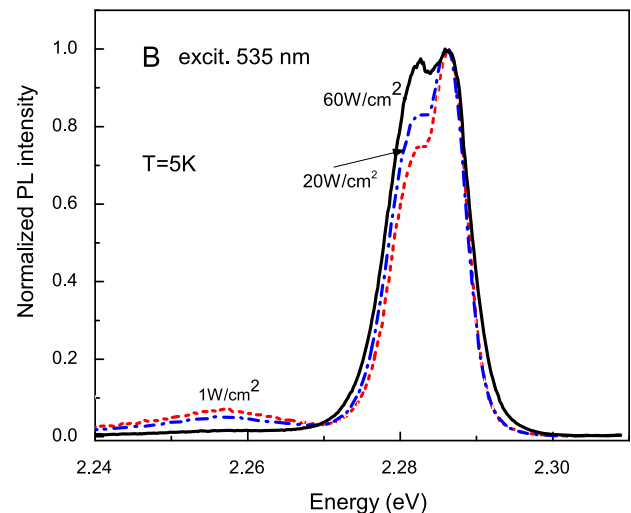
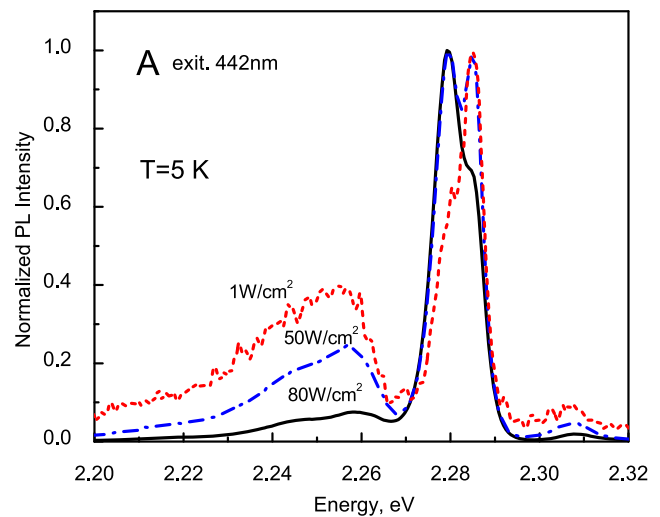


FIG. 2. (a) Normalized photoluminescence spectra at above the barrier optical excitation (442 nm) with intensities of $80\ \text{W}/\text{cm}^2$ (solid line), $50\ \text{W}/\text{cm}^2$ (dashed-dotted line), and $1\ \text{W}/\text{cm}^2$ (short-dashed line) and (b) normalized photoluminescence spectra at below-barrier optical excitation (535 nm) with intensities of $60\ \text{W}/\text{cm}^2$ (solid line), $20\ \text{W}/\text{cm}^2$ (dashed-dotted line), and $1\ \text{W}/\text{cm}^2$ (short dashed line).

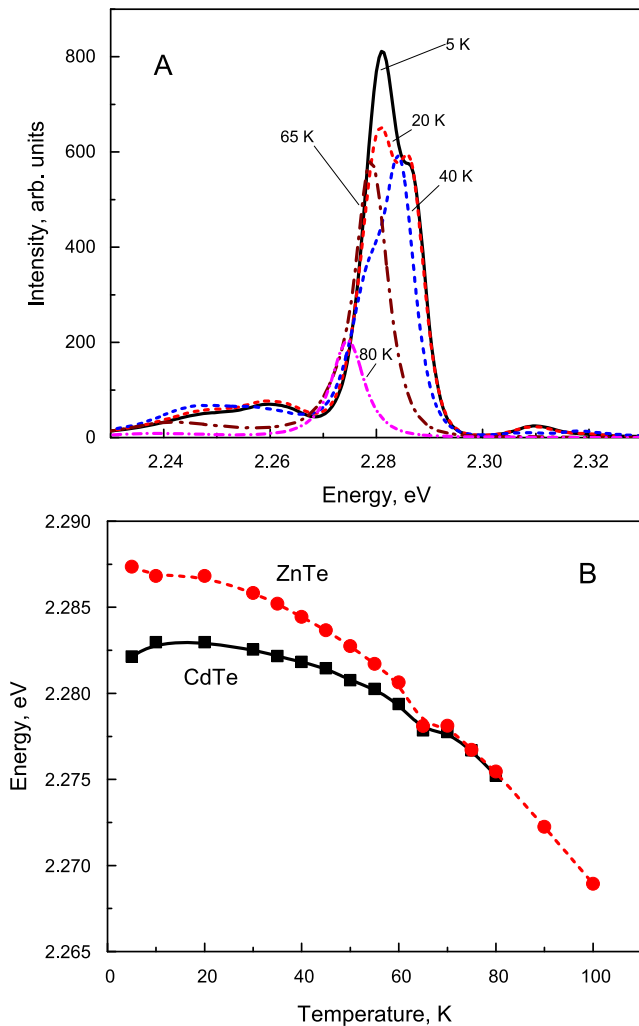


FIG. 3. Temperature dependence of photoluminescence spectra: (a) a set of the spectra taken at various temperatures, with an optical excitation intensity of ~ 60 W/cm 2 , and (b) temperature dependence of the energy positions of the exciton lines in the double quantum well.

one [Fig. 2(b)]. Under strong below-barrier excitation (~ 80 W/cm 2), the intensities of the doublet components equalize. In both cases, as the pumping increased, the PL maximum shifts toward the long-wavelength side. This behavior seems to be unusual since normally, the intensity redistributes in favor of the short-wave components with an increase in pumping due to the saturation of localized states.

Figure 2

An unusual behavior of the PL spectra was observed with temperature variation. With increasing temperature, the spectrum as a whole, as expected, shifts toward the long-wavelength side. However, the short-wave component of the doublet shifts faster than the long-wave one. As a result, the temperature dependences of line positions cross at a temperature of 60 K–65 K.

A nonmonotonic behavior of the intensities [Fig. 3(a)] and spectral positions [Fig. 3(b)] of the lines was observed in the intermediate region.

The total intensity of these lines decreases with increasing temperature, with their intensity redistributing from the short-wave component of the doublet to the long-wave one. As for the line widths, they change only slightly. The temperature dependences of the energy positions of the short-wave and long-wave components coincide with the temperature dependences of the band gap energies of ZnTe and CdTe, respectively. The temperature dependences of ZnTe and CdTe bandgaps are very similar. Nevertheless, one can distinguish them using the data of Refs. 10 and 11. Thus, these two components have to be connected with different layers of the structure and have a different nature.

Figure 3

The simple estimates of the energy splitting between these two lines show that this doublet cannot be symmetric and anti-symmetric states of the exciton in the double quantum well as the energy distance between the lines is too small. We suggest that the short-wave component is associated with a light hole exciton transition, whereas the long-wave component is associated with a heavy hole exciton one. The splitting of light and heavy exciton transitions in our structure can occur not only due to quantization but also due to mechanical stresses. Moreover, in CdTe/ZnTe structures, the light exciton is often displaced from the CdTe layers to the ZnTe layers.⁶ This fact explains the different temperature dependences of light and heavy exciton transition energies.

To verify this, the PL spectra obtained from the edge along the structure plane were analyzed. The selection rules in quantum wells are such¹² that the optical transitions involving a heavy exciton are polarized in the plane of the well whereas the transitions involving a light exciton have both polarization components. However, it turned

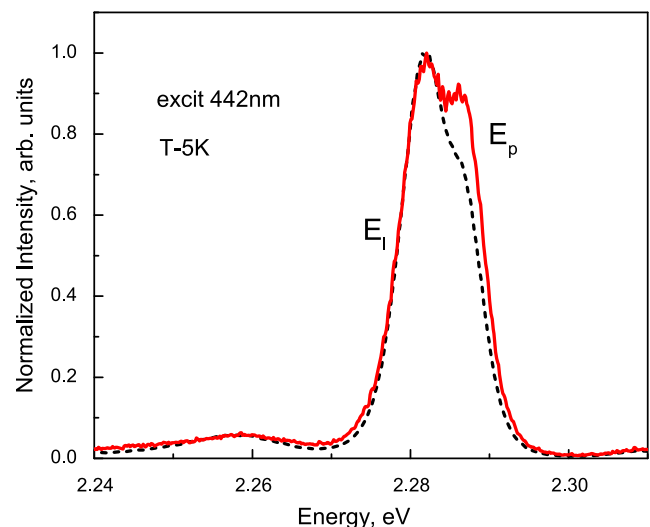


FIG. 4. Photoluminescence spectra normalized to the maximum at above-barrier excitation (442 nm) at 60 W/cm 2 , in linearly polarized light perpendicular to the layers (E_l) and parallel to the layers (E_p).

out that the waveguide effect is so strong in our structure that the PL signal with polarization along the CdTe layer was an order of magnitude greater than the perpendicular polarization. Nevertheless, the spectrum normalized to the maximum shows that the intensities of the doublet lines are equal in the polarization perpendicular to the well plane (Fig. 4). This partially confirms our interpretation of the short-wave line as a line of a heavy exciton and the long-wave one as a line of a light exciton.

Figure 4

However, these qualitative considerations do not elucidate the question concerning the exact light and heavy hole exciton line energy positions and their intensities. The problem is that the Bloch functions of the light and heavy hole states are such that the probability of transition from the light hole sub-band to the conduction band should be three times less than the probability of transition from the heavy hole sub-band for the light propagating perpendicular to the quantum well plane. As for our spectra, the intensities of these lines are approximately the same.

THEORY

Let us estimate the position of the light and heavy exciton levels in our structure. The lattice constants in ZnTe and CdTe materials differ by $\sim 7.8\%$. As a result, in addition to the potential associated with the so-called “chemical” band offset, the potential associated with mechanical stresses affects the carriers. The magnitude of the chemical band offset is known only approximately. This is especially true for ultrathin quantum wells, where the applicability of effective mass approximation is doubtful.³

Strictly speaking, it should not work well, but if the procedure is completed self-consistently, the result may be correct. The magnitude of the chemical band offset Δ is equal to the difference in the bandgaps of ZnTe and CdTe: $\Delta = E_g^{\text{ZnTe}} - E_g^{\text{CdTe}} = 0.78$ eV. This value is divided between the conduction band (Δ_c) and the valence band (Δ_v), $\Delta = \Delta_c + \Delta_v$. There have been many discussions and special measurements regarding Δ_c and Δ_v values,^{13–15} but the question still remains open. All existing measurements were carried out on fairly thick quantum wells. In this work, we, like other authors,^{16,17} will assume that $\Delta_c \gg \Delta_v$ and will consider Δ_c and Δ_v proportions according to our experimental data. Since the buffer layer and barrier ZnTe layers are thick, we can assume that these layers are totally relaxed and not stressed, whereas all mechanical stresses are located in the wells.

The deformation band offset can be calculated by^{18,19}

$$\begin{aligned} \delta E_c &= 2a_c(S_{11} + 2S_{12})\sigma, \\ \delta E_{hh} &= 2a_v(S_{11} + 2S_{12})\sigma + b(S_{11} - S_{12})\sigma, \\ \delta E_{lh} &= 2a_v(S_{11} + 2S_{12})\sigma - b(S_{11} - S_{12})\sigma. \end{aligned} \quad (1)$$

Here δE_c is the deformation band offset in the conduction band, δE_{hh} is the deformation offset in the heavy hole valence sub-band, δE_{lh} is the deformation offset of the light hole valence sub-band, a_c and a_v are the hydrostatic deformation potentials in the conduction and valence bands, respectively, b is the shear deformation potential, $S_{ij} \times 10^{-11} \text{ m}^2/\text{N}$ are the elastic constants, $\sigma = \frac{\epsilon}{(S_{11} + S_{12})}$ is the

mechanical tension perpendicular to the plane, and $\epsilon = \frac{a_j^t - a_i^t}{a_i^t}$ is the deformation perpendicular to the quantum well plane. For deformation potentials, the relations $a = a_c - a_v$ and $a_c/a_v = -2$ are valid^{20,21} (Table I).

Using formula (1), we obtain the strain induced offset in the conduction band and valence bands, which are presented in Table II

Consequently, the energy of a light hole in ZnTe layers is lower than its energy in CdTe layers, and as a result, the heavy exciton is related to CdTe layers and the light one is related to ZnTe layers.

In order to obtain the quantitative relations for the line intensities and their positions in the spectrum, we perform a full calculation of the exciton states in our structure. Since the sum of the chemical and the deformation band offset in the valence band in our structure is small, the Coulomb interaction with the electron becomes the main contributor to the potential energy of holes.^{22,24}

We assume that the electron and the hole move in δ -shaped potential wells [$V(z_e)$ for the electron and $V_0(z_h)$ for the hole], which are formed as a result of the offset between CdTe and ZnTe bands mentioned above and are coupled due to the electron–hole Coulomb interaction. The Schrödinger equation for the exciton has the following form:

$$\begin{aligned} & \left[-\frac{\hbar^2}{2m_e} \frac{\partial^2}{\partial z_e^2} + V(z_e) - \frac{\hbar^2}{2m_h} \frac{\partial^2}{\partial z_h^2} + V_0(z_h) \right. \\ & \left. - \frac{\hbar^2}{2\mu} \left(\frac{1}{\rho} \frac{\partial}{\partial \rho} \rho \frac{\partial}{\partial \rho} + \frac{1}{\rho^2} \frac{\partial^2}{\partial \phi^2} \right) - \frac{e^2}{\epsilon_0 \sqrt{\rho^2 + |z_e - z_h|^2}} \right] \Psi(\mathbf{r}_e, \mathbf{r}_h) \\ & = \left(E - \frac{\hbar^2 Q_1^2}{2M} \right) \Psi(\mathbf{r}_e, \mathbf{r}_h). \end{aligned} \quad (2)$$

Here, $\phi = \arctg\left(\frac{x_e - x_h}{y_e - y_h}\right)$, $\rho = \sqrt{|x_e - x_h|^2 + |y_e - y_h|^2}$, and $V(z_e) = -\gamma\left[\delta\left(z_e - \frac{R}{2}\right) + \delta\left(z_e + \frac{R}{2}\right)\right]$ for electrons, $V_0(z_h) = -\eta\left[\delta\left(z_h - \frac{R}{2}\right) + \delta\left(z_h + \frac{R}{2}\right)\right]$ for holes, γ and η are strength of the δ -shaped potential (at the first order, they are equal to the product of the band offset and the lattice constant), R is the distance between two quantum wells, Q_1 is the exciton wave vector in the plane of the structure, and E is the exciton total energy.

TABLE I. Deformation potentials and elastic constants in CdTe.

S_{11}	S_{12}	S_{44}	a (eV)	b (eV)	σ
3.581	−1.394	5.5	−3.85	−1.20	0.0358

TABLE II. Deformational band offset for the CdTe/ZnTe heterostructure.

δE_c (meV)	δE_{hh} (meV)	δE_{lh} (meV)
−150	−20	+165

We assume that the electronic subsystem is “fast,” i.e., $\frac{\hbar^2 p^2}{m_e} \gg \frac{e^2}{\epsilon_0 \tilde{a}_B}$ (the electron kinetic energy in the well is greater than the potential energy of its interaction with a hole in the exciton), $1/l$ is the effective width of $V(z_e)$, and \tilde{a}_B is the Bohr radius of the exciton in the plane of the quantum well (we will consider it as a variational parameter). Then, one can first solve the equation for the electron motion in the z direction and then solve the equation for the hole motion in the averaged field created by the electron. In this case, we can write the exciton wavefunction as $\Psi(\mathbf{r}_e, \mathbf{r}_h) = f(\rho, \phi) \varphi_e(z_e) \varphi_h(z_h)$. Here, $f(\rho)$ is the wavefunction of the internal motion of the 2D exciton, $\varphi_e(z_e)$ is the wavefunction of an electron in the z direction, and $\varphi_h(z_h)$ is the wavefunction of an electron in the z direction.

The equation for electron motion in the z direction is as follows:

$$\left[-\frac{\hbar^2}{2m_e} \frac{\partial^2}{\partial z_e^2} + V(z_e) - E_e \right] \varphi_e(z_e) = 0. \quad (3)$$

The solution of this equation in our potential for the symmetric state looks as follows:

$$\varphi_e(z_e) = A \left[e^{-d|z_e + \frac{R}{2}|} + e^{-d|z_e - \frac{R}{2}|} \right], \quad (4)$$

where A is the normalized constant and $1/d$ is the size of the electron wave function in the z direction.

The energy of the electron ground state in the double δ -shaped well can be written as

$$E_e = -\frac{\hbar^2}{2m_e} d_+^2, \quad d_+ = \frac{m}{\hbar^2} \gamma (1 + e^{-d_+ R}). \quad (5)$$

The antisymmetric state, with $d_- = m\gamma(1 - e^{-d_- R})/\hbar^2$, is unbound.

At the second step, it is necessary to solve the equation for the 2D exciton and consider the equation for the hole motion in the average potential created by the electron. The equation for a 2D exciton is

$$\left[-\frac{\hbar^2}{2\mu} \left(\frac{1}{\rho} \frac{\partial}{\partial \rho} \rho \frac{\partial}{\partial \rho} + \frac{\partial^2}{\partial \phi^2} \right) - \frac{e^2}{\epsilon_0 \rho} - E_{2D}^{exc} \right] f_n(\rho, \phi) = 0. \quad (6)$$

The solution for the ground state is

$$f_1(\rho, \phi) = \sqrt{\frac{2}{\pi}} \frac{1}{\tilde{a}_B} e^{-\frac{\rho}{\tilde{a}_B}}. \quad (7)$$

Here $\tilde{a}_B = a_B/2$ is the 2D exciton Bohr radius, and a_B is the Bohr radius of the 3D exciton, given by

$$a_B = \frac{\epsilon_0 \hbar^2}{\mu e^2} = \sqrt{\frac{\hbar^2}{2\mu E_{3D}^{exc}}}. \quad (8)$$

2D exciton Rydberg energy is

$$E_{2D}^{exc} = -\frac{\mu e^4}{2\hbar^2 \epsilon_0^2} \frac{1}{(n - 1/2)^2}. \quad (9)$$

The effective potential acting on the hole has the following form:

$$V_{eff}(z_h) = V_0(z_h) - \frac{e^2}{\epsilon_0} \frac{2}{\pi} \frac{d^c}{\tilde{a}_B^2} \int_{-\infty}^{\infty} dz_e |\varphi_c(z_e)|^2 \times \int_0^{\infty} \rho d\rho e^{-2\rho/\tilde{a}_B} \left[-\frac{1}{\rho} + \frac{1}{\sqrt{(\rho^2 + (z_e - z_h)^2)}} \right]. \quad (10)$$

TABLE III. Effective masses in CdTe and ZnTe. The 3D exciton Bohr radius in CdTe is $a_B = 61.9 \text{ \AA}$.^{20,a}

	m_e	m_{hh}	m_{lh}
CdTe	0.094	0.72	0.13
ZnTe	0.12	0.83	0.15

^aThe masses were taken from the Luttinger parameters.

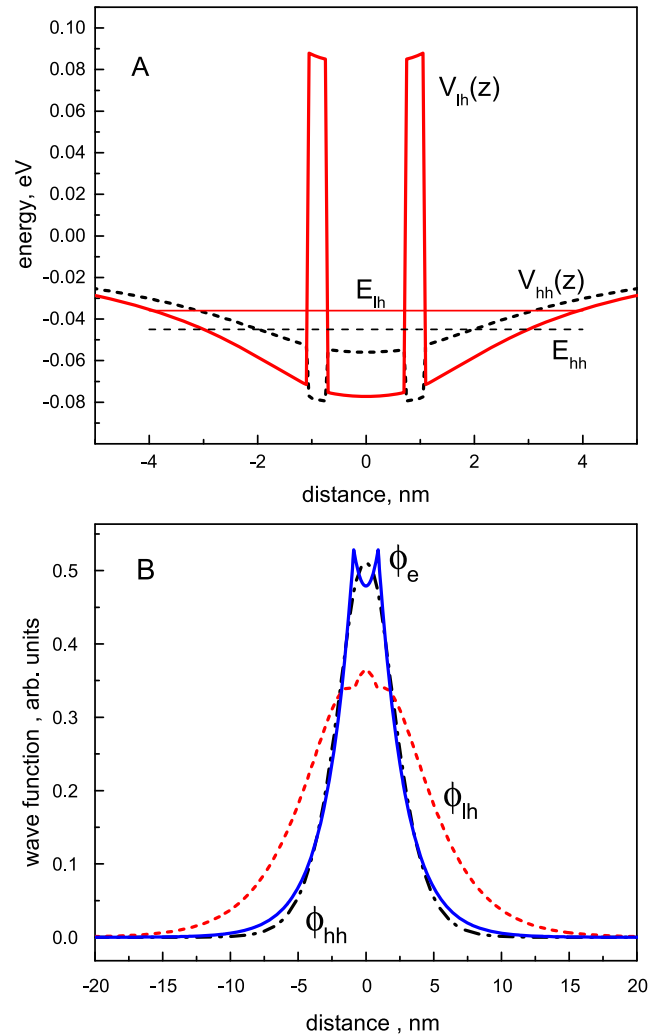


FIG. 5. Calculation of the effective potential for the hole motion $V_{eff}(z_h)$ created by an electron in a double δ -shaped quantum well and the wave functions of holes $\varphi_h(z_h)$ (scheme): (a) effective potentials $V_{eff}(z_h)$ for the heavy hole $V_{hh}(z)$ (solid line) and the light hole $V_{lh}(z)$ (short dashed line). The energy levels of the heavy hole E_{hh} (short-dashed line) and the light hole E_{lh} (dashed-dotted line) in the effective field of the electron and (b) the wave functions of the electron (solid line) $\varphi_e(z_e)$ of the heavy hole (dashed-dotted line) $\varphi_{hh}(z_h)$ and the light hole (dashed line) $\varphi_{lh}(z_h)$.

We used \tilde{a}_B as variational parameter to minimize the total exciton energy. At the last step, we find the energy levels and wave functions of the heavy and light holes for this potential. The parameters used in our calculation are shown in Table III.

The energy levels and wave functions of the heavy and light excitons were calculated numerically by solving the Schrödinger equation for the exciton (2) using the finite elements method. The result of the calculation is shown in Fig. 5.

The magnitude of the band offset in the conduction band is quite large (not less than 600 meV). As a result, the size of the electron wave function along the z direction in the δ -shaped potential is insensitive to the exact value of the strength γ of this potential. We took the strength of the potential as $\gamma = 3.9$ (eV Å). Knowing the potential strength, we can find the “size” of the wave function along the z direction ($1/d_+$) in the double quantum well. For an electron, it is $d_+^e = 0.07$ (Å⁻¹). This is enough to calculate the Coulomb potential acting on the hole (10). By minimizing the heavy and light exciton energies, we found the exciton Bohr radius \tilde{a}_B and the difference between heavy and light hole energies. To find the value of η and, consequently, one of the valence band discontinuities, we fit the experimental and calculated differences between heavy and light exciton energies.

Figure 5

The calculation showed that the energy position of the light exciton level is practically independent of the bandgap and is “tied” to the valence band of ZnTe. At the same time, the energy position of the heavy exciton level linearly depends on the band offset and is “tied” to the CdTe band. It is this fact that explains the different temperature dependences of the position of the heavy and light exciton levels (Fig. 3).

We achieved the best agreement between the calculated and experimentally measured energies of light and heavy excitons by varying the magnitude of the valence band offset.

As a result, the value of the total band offset in the valence band was found. Knowing the magnitude of the total and deformation band offsets, we can determine the chemical band offset in the valence band in a CdTe/ZnTe system, the strength of the potential, and the size of the wave function. The chemical band offsets in the valence band turned out to be ~ 10 meV, which is equal to 2% of the total chemical band offset.

DISCUSSION

In our structures, the potential for electrons is narrow and deep. However, despite the fact that the electron quantization energy in this potential is several hundred meV, due to the small mass of the electron, the penetration of its wave function into the barriers is spread over $1/d \approx 20$ Å. This value is of the same order as the distance between the CdTe quantum wells, that is, the wells are coupled to each other by the common electron wave function and should be considered as a whole. The lowest energy state (symmetric state) is even with respect to the reflection in a plane passing through the middle between the wells. The upper energy state (anti-symmetric) should be odd, but in our case, it is lying above the barriers.

The strength of the heavy hole potential is about 10 times less than the strength of the electron potential, and therefore, the quantization energy should be even less. However, the effective mass of the heavy hole perpendicular to the quantum well plane is 8 times larger than the mass of the electron. As a result, the penetration depth of the heavy hole wave function into the barriers is only 3 times larger than the electron penetration, that is, $1/d \approx 70$ Å.

For the light hole, a type II structure is predicted due to mechanical stresses. The light hole is forced into ZnTe layers limited by δ -shaped CdTe barriers with a height of about 150 meV. However, due to the small thickness of these barriers, the tunneling probability of light holes is large, and it can be considered almost free in the ZnTe matrix.

Thus, the main factor determining the energy levels and wave functions of the holes in our structure is their Coulomb interaction with the electrons. In this case, the energy and wave functions of an electron are mainly determined by its quantization in a δ -shaped double well since the quantization energy of the electron is many times greater than its Coulomb energy.

As known from Luttinger Hamiltonian, a heavy hole has a small mass in the plane of the quantum well and vice versa—a light hole has a large mass in the plane of the well. As a result, the Bohr radius of the light exciton in the two-dimensional approximation \tilde{a}_B is ~ 1.7 times smaller than the Bohr radius of the heavy exciton. Therefore, the binding energy of a light exciton in the 2D approximation is 1.7 times larger than the binding energy of a heavy exciton.

The oscillator strength of the 2D exciton^{12,23} is inversely proportional to the square of its Bohr radius and proportional to the square of the overlap integral of the electron and hole wave functions. It turned out that the overlap integral along the z axis for the electron and the light hole is approximately equal to the overlap integral for the electron and the heavy hole. The large value of the light hole overlap integral is due to the fact that its energy in the δ -shaped barriers is higher than its energy in the gap between them. It seems to be «absorbed» into the area between the barriers due to the repulsive nature of the barrier potential.

The heavy hole, on the contrary, is «pushed» out from the Coulomb field of the electron by an attractive barrier potential since its energy in the δ -shaped barriers is lower than the energy between them (Fig. 5). As a result, despite the fact that the interband matrix element of the dipole moment of the optical transition for the heavy hole is 3 times larger than that for the light hole, due to the larger overlap of wave functions, the oscillator strength of the light exciton turned out to be comparable with the oscillator strength of the heavy exciton, in accordance with our experiment.

An above-barrier excitation, in contrast to the below-barrier one, leads to the charge of residual impurity centers in ZnTe layers. The electric field of charged impurities can change the potential for holes in the valence band. This, in turn, can lead to a modification in hole and electron overlaps and, as a result, to a redistribution of the intensity of light and heavy exciton lines.

The different temperature dependences of the light and heavy exciton energy are explained by the fact that the light hole is “displaced” into ZnTe layers and thin CdTe barriers have almost no effect on its energy while the heavy hole is localized due to CdTe layers and its energy is entirely related to the CdTe band.

From the calculation of the wave functions, it was found that the oscillator strength of the light exciton transition is equal to that

of the heavy exciton one, with an accuracy of 15%. The binding energy of a light exciton turned out to be even slightly larger than the binding energy of a heavy exciton.

CONCLUSION

In this work, we studied the reflection and PL spectra of CdTe/ZnTe structures with double δ -like quantum wells. The heavy and light excitons lines are identified. These lines have different temperature dependences, clearly indicating that the heavy exciton is mainly located in the CdTe layers and the light one is in the ZnTe layers.

The intensities of the heavy and light exciton transitions turned out to be approximately the same, which is a fingerprint that the wave function overlap of the light hole and the electron is noticeably larger than the one between the heavy hole and the electron. The calculation of energy levels and wave functions of heavy and light excitons confirms our interpretation of the lines. Based on the results of fitting the calculation to the experiment, the chemical band offset for monolayer CdTe inclusions in the ZnTe matrix turned out to be 2% of the total chemical band offset.

AUTHORS' CONTRIBUTIONS

N.G.F., A.Yu.S., and V.F.A. made experimental measurements, N.G.F. performed calculations, G.K. grew samples, and V.P.K. and H.M. interpreted the experimental data and the idea of the paper and wrote the paper.

ACKNOWLEDGMENTS

The equipment of St. Petersburg State University Science Park was used as a part of the INI_2019 project, ID No.: 37688845. The research in Poland was partially supported by the National Science Centre through Grant Nos. 2017/25/B/ST3/02966 and 2018/30/M/ST3/00276.

DATA AVAILABILITY

The data that support the findings of this study are available from the corresponding author upon reasonable request.

REFERENCES

- ¹H. Mathieu, J. Allegre, A. Chatt, P. Lefebvre, and J. P. Faurie, "Band offsets and lattice-mismatch effects in strained-layer CdTe/ZnTe superlattices," *Phys. Rev. B* **38**(11), 7740 (1988).
- ²D. J. Dunstan, A. D. Prins, B. Gil, and J. P. Faurie, "Phase transitions in CdTe/ZnTe strained layer superlattices," *Phys. Rev. B* **44**(8), 4017 (1991).
- ³C. Priester, G. Allan, and M. Lannoo, "Ultra-thin semiconductor quantum wells: Potential shapes and strain effects," *J. Physique Colloq.* **48**(C5), C5-203–C5-206 (1987).
- ⁴V. F. Agekyan, A. Y. Serov, N. G. Filosofov, I. V. Shtrom, and G. Karczewski, "Optical properties of zinc telluride with cadmium telluride submonolayers," *Phys. Solid State* **58**, 2109 (2016).

- ⁵R. Cingolani, O. Brandt, L. Tapfer, G. Scamarcio, G. C. La Rocca, and K. Ploog, "Exciton localization in submonolayer InAs/GaAs multiple quantum wells," *Phys. Rev. B* **42**, 3209(R) (1990).
- ⁶H. Tuffigo, N. Magnea, H. Mariette, A. Wasiela, and Y. Merle d'Aubigné, "Optical investigation of a strain-induced mixed type-I–type-II superlattice system: CdTe/Cd_xZn_{1-x}Te," *Phys. Rev. B* **43**(18), 14629 (1991).
- ⁷H. Kalt, J. Collet, S. D. Baranovskii, R. Saleh, P. Thomas, L. S. Dang, and J. Cibert, "Optical- and acoustical-phonon-assisted hopping of localized excitons in CdTe/ZnTe quantum wells," *Phys. Rev. B* **45**, 4253 (1992).
- ⁸I. Hernández-Calderón, M. García-Rocha, and P. Díaz-Arencibia, "Growth and characterization of ultra-thin quantum wells of II–VI semiconductors for optoelectronic applications," *Phys. Status Solidi B* **241**, 558 (2004).
- ⁹G. Lentz, A. Ponchet, N. Magnea, and H. Mariette, "Growth control of CdTe/CdZnTe (001) strained-layer superlattices by reflection high-energy electron diffraction oscillations," *Appl. Phys. Lett.* **55**, 2733 (1989).
- ¹⁰R. Pässler, "Semi-empirical description of temperature dependences of band gaps in semiconductors," *Phys. Status Solidi B* **236**(3), 710 (2003).
- ¹¹R. Pässler, E. Griehl, H. Riepl, G. Lautner, S. Bauer, H. Preis, W. Gebhardt, B. Buda, D. J. As, D. Schikora, K. Lischka, K. Papagelis, and S. Ves, "Temperature dependence of exciton peak energies in ZnS, ZnSe, and ZnTe epitaxial films," *J. Appl. Phys.* **86**(8), 4403 (1999).
- ¹²E. L. Ivchenko, *Optical Spectroscopy of Semiconductor Nanostructures* (Alpha Science International Limited, Harrow, UK, 2005).
- ¹³E. Deleporte, J. M. Berroir, G. Bastard, C. Delalande, J. M. Hong, and L. L. Chang, "Magnetic-field-induced type-I–type-II transition in semimagnetic CdTe/Cd_{0.93}Mn_{0.07}Te superlattice," *Phys. Rev. B* **42**(9), R5891 (1990).
- ¹⁴E. Deleporte, J. M. Berroir, C. Delalande, N. Magnea, H. Mariette, J. Allegre, and J. Calatayud, "Excitonic effects in separate confinement quantum well heterostructures CdTe/(Cd,Zn)Te," *Phys. Rev. B* **45**(11), R6305 (1992).
- ¹⁵S. V. Zaitsev, I. V. Sedova, S. V. Sorokin, and S. V. Ivanov, "Magneto-optics of (Zn,Cd,Mn)Te/ZnTe heterostructures with a small potential gap in the valence band," *JETP Lett.* **88**, 802 (2008).
- ¹⁶T. N. Zavaritskaya, I. V. Kucherenko, N. N. Mel'nik, G. Karczewski, and M. L. Skorikov, "Photoluminescence and exciton resonances over the scattered light in multiphonon spectra of resonant scattering in the CdTe/ZnTe superlattices with narrow quantum wells," *Phys. Solid State* **55**, 2355 (2013).
- ¹⁷V. I. Kozlovskii, V. G. Litvinov, and Y. G. Sadofev, "Band offsets in Zn_{1-x}Cd_xTe/ZnTe single-quantum-well structures grown by molecular-beam epitaxy on GaAs (001) substrates," *Semiconductors* **34**, 960 (2000).
- ¹⁸L. S. Dang, J. Cibert, Y. Gobil, K. Saminadayar, and S. Tatarenko, "Optical study of residual strain in CdTe and ZnTe layer grown by molecular beam epitaxy," *Appl. Phys. Lett.* **55**(3), 235 (1989).
- ¹⁹H. Mariette, F. Dal'bo, N. Magnea, G. Lentz, and H. Tuffigo, "Optical investigation of confinement and strain effects in CdTe/Cd_{1-x}Zn_xTe single quantum wells," *Phys. Rev. B* **38**(17), 12443 (1988).
- ²⁰*Landolt-Bornstein: Numerical Data and Functional Relationship in Science and Technology*, Group III: Condensed Matter, edited by W. Martienssen (Springer, 2000).
- ²¹P. Peyla, Y. Merle d'Aubigné, A. Wasiela, R. Romestain, H. Mariette, M. D. Sturge, N. Magnea, and H. Tuffigo, "Exciton binding energies and the valence-band offset in mixed type-I–type-II strained-layer superlattices," *Phys. Rev. B* **46**(3), 1557 (1992).
- ²²N. T. Pelekanos, P. Peyla, L. S. Dang, H. Mariette, P. H. Jouneau, A. Tardot, and N. Magnea, "Ultrathin pseudomorphic layers of ZnTe in CdTe/(Cd,Zn)Te superlattices: A direct optical probe of the mixed-type band configuration," *Phys. Rev. B* **48**(3), 1517 (1993).
- ²³J. Feldmann, G. Peter, E. O. Gobel, P. Dawson, K. Moore, C. Foxon, and R. J. Elliott, "Linewidth dependence of radiative exciton lifetime in quantum wells," *Phys. Rev. Lett.* **59**, 2237 (1987).
- ²⁴A. L. Efros, "Excitons in quantum-well structures," *Sov. Phys.: Semicond.* **20**, 808 (1986).